Eur. Phys. J. D **15**, 155–164 (2001)

THE EUROPEAN PHYSICAL JOURNAL D

EDP Sciences

The positronium negative ion: Classical properties and semiclassical quantization

N.S. Simonović[a] and J.M. Rost

Max-Planck-Institute for the Physics of Complex Systems, Nöthnitzer Str. 38, 01187 Dresden, Germany

Received 19 January 2001

Abstract. Properties of collinear and planar periodic orbits for the positronium negative ion are examined with respect to the possibilities for semiclassical quantization. In contrast to other two-electron atomic systems as helium and H^- the relevant orbits for quantization are fully stable and permit a full torus quantization. However, for lower excitations the area of stability in phase-space is too small for a reliable torus quantization. Instead, a quasi-separability of the three-body system is used to apply effective one-dimensional (WKB) quantization.

PACS. 36.10.-k Exotic atoms and molecules (containing mesons, muons, and other unusual particles) – 31.50.+w Excited states – 03.65.Sq Semiclassical theories and applications

1 Introduction

Electron correlation in two-electron systems, particularly for doubly excited states, has been studied for a long time within different frameworks [1]. Semiclassical methods provide a systematic approximation to the resonance spectrum on the one hand side [2]. On the other side the first term of the expansion of the Greens function into periodic orbit contributions, namely the *collinear* so-called asymmetric stretch (AS) orbit, leads to a simple yet fairly accurate approximation of symmetrically excited ("intra-shell") resonances with a clear physical picture [1,3]. Yet, an alternative description, the so-called asynchronous model, has been developed by Simonović and Grujić [4] in terms of *planar* orbits which are obviously higher dimensional objects in phase space. Due to the quasi separability of the three-body Coulomb problem [1], they are nevertheless easily computed. It has been shown that for atoms (helium [4]) and for negative ions (H^- [5]), *i.e.* for systems with a heavy positive core, the asynchronous and the AS orbits yield roughly the same resonance positions over a wide energy range upon semiclassical quantization for excitation along the AS orbit. This may be surprising on a first glance since for each resonance, a different asynchronous orbit is quantized, while in the AS approximation it is a single orbit which is responsible for all quantized states. Consequently, resonances which correspond to excitations perpendicular to the AS orbit (so-called bending vibrations) are poorer represented in the AS description, which is collinear only, compared to the planar asynchronous orbits.

That the quantitative semiclassical results are rather similar in both approaches despite the use of different orbits could be attributed partially to the fact that all these orbits have similar global properties, *i.e.*, they are unstable.

Our motivation for the semiclassical investigation of the positronium negative ion (Ps^-) is driven by the observation that the AS orbit for this system is *stable* [6]. Are all the asynchronous orbits underlying the resonances also stable? As it will turn out not all of them are stable. Ps^- has been studied experimentally as well as theoretically, where in the latter case emphasis was put on the question what kind of energy spectrum this peculiar three-body system with three particles of equal mass might possess. Only recently, it was demonstrated that not only zero angular momentum resonances are ordered quite similarly to that of H^- [7], but that also the ro-vibrational spectrum as a whole exhibits similar features as the one of H^- [8]. The quantum mechanical similarity makes it even more interesting to see if it is preserved semiclassically, despite the different stability properties of the underlying classical orbits.

The paper is organized as follows: in Section 2 we introduce the Hamiltonian and describe briefly how we determine the classical orbits. In Section 3 we describe the relevant classical configurations and discuss the quasi-separability which is apparent from these orbits. Section 4 presents the semiclassical quantization procedure for the different cases along with the results. The paper concludes with a short summary in Section 5.

2 The Hamiltonian

In relative coordinates r_i, pointing from the positron to the two electrons, respectively, the Hamiltonian for Ps^-

[a] e-mail: nenad@mpipks-dresden.mpg.de

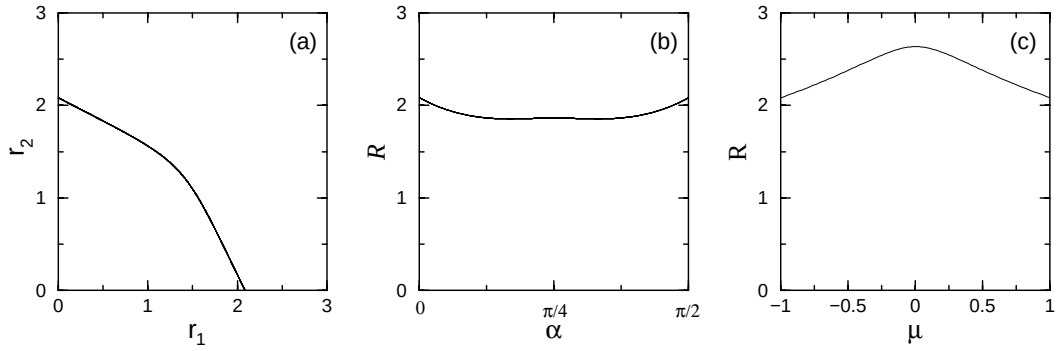

Fig. 1. The AS PO for the Ps^-, (a) in independent particle coordinates r_1, r_2, (b) in hyperspherical coordinates $\mathcal{R}$, α and (c) in molecular coordinates $R = r_{12}$, $\mu = (r_1 - r_2)/R$. The full action of the AS orbit for Ps^- (at $E = -1$) is $S = S_0 \equiv 7.2151$ (then $S_1 = S_2 = 0$ and $S_3 = S_0$). The corresponding winding numbers, evaluated from its monodromy matrix [14], are $\gamma_1^{(0)} = 1.11622$, $\gamma_2^{(0)} = 0.62978$.

reads

$$H = \mathbf{p}_1^2 + \mathbf{p}_2^2 + \mathbf{p}_1 \cdot \mathbf{p}_2 - \frac{1}{r_1} - \frac{1}{r_2} + \frac{1}{r_{12}}, \qquad (1)$$

where $r_{12} = |\mathbf{r}_1 - \mathbf{r}_2|$ and $\mathbf{p}_i$ are the momenta conjugated to $\mathbf{r}_i$. Since equations of motion for Coulombic systems are invariant under a continuous similarity transformation [9] it is sufficient to carry out all calculations at fixed energy $E = -1$. For example, if S is the action along a trajectory calculated at $E = -1$, the energy of the scaled trajectory with action S' is $E' = -(S/S')^2$. This property is particularly important for a semiclassical quantization of Coulomb systems, because it significantly simplifies the procedure.

The potential in (1) has attractive singularities at $r_i = 0$, $i = 1, 2$. Hence, a regularization of the equations of motion must be performed before they can be solved numerically. Here, we follow the procedure by Aarseth and Zare (see Appendix), originally introduced to regularize the three-body problem in celestial mechanics [10].

3 Quantum mechanically relevant classical configurations

The two fundamental collinear periodic orbits (POs) of a two-electron system are the symmetric stretch (SS) and the asymmetric stretch (AS) POs. They represent in-phase and out-of-phase motion, respectively. Beside these, there is an infinite set of collinear periodic orbits which may be considered as representing the coupling of the SS and AS fundamental modes [11]. WKB quantization of the AS periodic orbit in the case of helium gives reasonably accurate results for the doubly-excited intra-shell resonances ($N = n$), but for the states with $N \neq n$ the contribution of other periodic orbits is essential[1]. A comparison with quantum probability distributions also suggests to associate the AS orbit with the intra-shell resonances rather than the SS [3,13].

[1] For such states a more sophisticated semiclassical approach is necessary, *e.g.* the Gutzwiller's PO theory [12].

As we mentioned above, in contrast to the previously considered two-electron atomic systems (He, H^-), the collinear AS orbit for Ps^- and the orbits in its vicinity are fully stable [6], *i.e.* there are three stable oscillatory modes: the (principal) asymmetric stretch (AS) mode, the symmetric stretch (SS), and the bending modes. The bending mode has kinetic energy dominantly in the interelectronic angle ϑ_{12}, in contrast to the collinear modes for which $\vartheta_{12} = 180°$. In the case of angular momentum $L = 0$ which we consider here, the motion is confined to invariant tori in 6-dimensional phase-space. This dynamics is conveniently described by hyperspherical coordinates, *i.e.*, with hyperradius $\mathcal{R} = (r_1 + r_2)^{1/2}$, hyperangle $\alpha = \arctan(r_2/r_1)$ and the interelectronic angle $\vartheta_{12} = \vartheta_1 - \vartheta_2$ (here we use the same set as it is defined for He and H^-, but the canonically conjugated momenta $p_{\mathcal{R}}$, p_α and $p_{\vartheta_{12}}$ are different). In Figure 1, the AS PO for the Ps^- is shown in three different coordinate systems. The three fundamental modes SS, AS, and bending, correspond in hyperspherical coordinates to motion along $\mathcal{R}$, α and ϑ_{12} (perpendicular to the plane shown in Fig. 1), respectively. This correspondence is, however, only approximate which is reflected, for example, in small oscillation of the hyperradius for the AS orbit (see Fig. 1b), although in this case, neither the SS-mode nor the bedding modes are excited.

Trajectories in the vicinity of the collinear AS periodic orbit are characterized by two winding numbers defined by the ratios

$$\gamma_1 = \frac{\omega_1}{\omega_3}, \quad \gamma_2 = \frac{\omega_2}{\omega_3}, \qquad (2)$$

where ω_1, ω_2 and ω_3 are the characteristic frequencies of the bending, SS and AS modes, respectively. They, actually, label the invariant tori on which these stable trajectories lie. Apart from the frequencies, each torus is defined by three action integrals I_i along topologically distinct paths (they need not necessarily be classical trajectories) with

$$I_i = \frac{1}{2\pi} \oint_{c_i} (\mathbf{p}_1 \cdot \mathrm{d}\mathbf{r}_1 + \mathbf{p}_2 \cdot \mathrm{d}\mathbf{r}_2), \quad i = 1, 2, 3, \qquad (3)$$

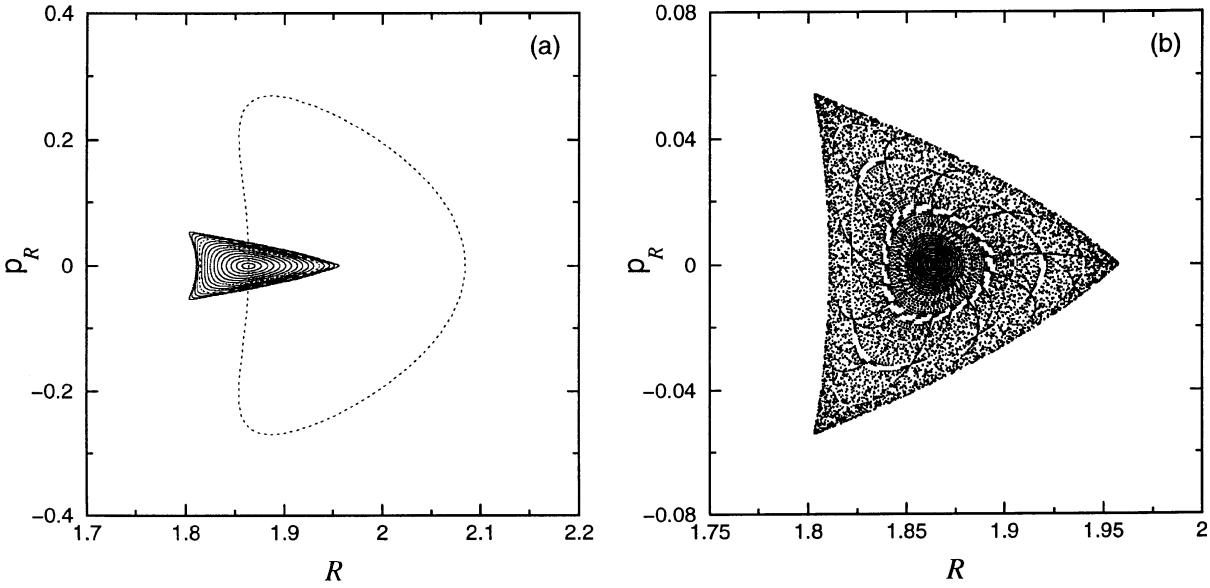

Fig. 2. The stability island around the AS collinear PO for Ps^- in the AS–SS symmetry plane visualized by the Poincaré surface of section $\{(\mathcal{R}, p_\mathcal{R})|\alpha = \pi/4, p_\alpha > 0\}$: (a) 17 orbits $x_2 \in (2.084, 2.004)$, $t \leq 5\,000$ (dotted line is the $\mathcal{R}$-component of the AS PO in phase space); (b) 82 orbits $x_2 \in (2.084, 2.003)$, $t \leq 500$.

where the paths c_1, c_2, c_3 are along bending, SS and AS modes, respectively. Since the full action accumulated in time t along a trajectory on the torus is $S(t) = \sum_i \omega_i I_i$, the action accumulated over one period of the AS-mode T_3 is

$$S \equiv S(T_3) = \gamma_1 S_1 + \gamma_2 S_2 + S_3, \tag{4}$$

where $S_i = 2\pi I_i$. Hence, alternatively, each torus can be labeled by three actions S, S_1, S_2. Moreover, if all trajectories are calculated at fixed energy $E = -1$, then $S = S(S_1, S_2)$ and the corresponding (scaled) tori are labeled by two actions S_1 and S_2, which tell us how far away from the AS the trajectories on these tori are in phase space. These properties will be used below for the semiclassical quantization of the system.

There exist, however, invariant subspaces of the full phase-space where the three-dimensional motion essentially reduces to two degrees of freedom (so-called symmetry planes [15]). If we consider the bound motion with two of the three oscillatory modes excited, the invariant subspaces are: (i) AS–SS, (ii) AS-bending and (iii) SS-bending. The AS–SS subspace represents collinear orbits ($S_1 = 0$) with the AS-radial motion as the principal mode and small excitations of the SS-mode (*i.e.* the collinear configuration with electrons on the opposite sides of the positron, denoted by $e^-\mathrm{Ze}^-$ in [15]). In the AS-bending subspace the orbits are planar and have been named "asynchronous orbits" [4,5]. They have no excitation in the SS-mode ($S_2 = 0$). Finally, the third subspace is the so-called Wannier ridge [11] containing the orbits with $r_1 = r_2$ at all times (then $S_3 = 0$). Since the motion is stable in the vicinity of the AS PO, the cases of interest are (i) and (ii).

3.1 The collinear configurations (AS–SS subspace)

Stable orbits for the Ps^- system within the AS–SS subspace are computed (at total energy $E = -1$ and total angular momentum $L = 0$) starting from initial collinear configuration with electron-positron distances $x_1^{\mathrm{in}} = 0$, $x_2^{\mathrm{in}} \in (2.00236, 2.08425)$. The value $x_2^{\mathrm{in}} = 2.08425$ corresponds to the AS PO, whereas for $x_2^{\mathrm{in}} < 2.00236$ the orbits become chaotic. As pointed out in [6], the area of stability for these SS-excitations is rather small ($\Delta\mathcal{R}/\mathcal{R} < 0.05$). This can be seen from Figure 2, where the stability island around the AS PO in the AS–SS subspace is made visible by the help of the Poincaré surface of section $\{(\mathcal{R}, p_\mathcal{R})|\alpha = \pi/4, p_\alpha > 0\}$. For irrational tori within this subspace (γ_2 irrational) the actions S_2 are the areas enclosed by the corresponding curves in the section. The area enclosed by the boundaries of the stability island is $S_2^{\max} \approx 0.009$.

3.2 The asynchronous configurations (AS-bending subspace)

These configurations are 2-dimensional extensions of the 1-dimensional collinear AS configuration, obtained by including the bending mode but without any SS-motion (*i.e.* $S_2 = 0$). However, small oscillations of the hyper-radius $\mathcal{R}$ exist nevertheless due to the coupling of the motion in α and ϑ_{12}. The asynchronous orbits for the Ps^- system can be computed (at $E = -1$ and $L = 0$) starting with initial momenta $(\mathbf{p}_1^{\mathrm{in}}, \mathbf{p}_2^{\mathrm{in}})$ perpendicular to the initial collinear configuration with electron-positron distances $(x_1^{\mathrm{in}}, x_2^{\mathrm{in}})$ connected by the full lines in Figure 3. Note that bifurcation points appear around the values $x_1^{\mathrm{in}} = 0.115$ and $x_1^{\mathrm{in}} = 0.217$ rendering the orbits in its vicinity chaotic. The orbits also become highly chaotic for $x_1^{\mathrm{in}} > 0.225$.

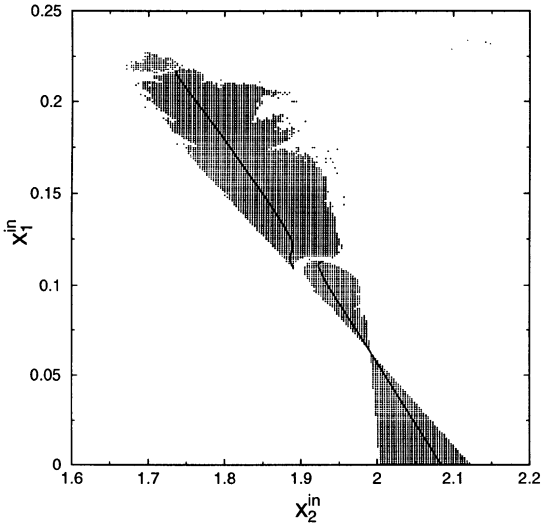

Fig. 3. The stable area of the initial configuration space for Ps^-. The initial electron-positron distances (x_1^{in}, x_2^{in}) for the asynchronous orbits from the AS-bending subspace are connected by full lines. The configuration is fully stable in the wide range from $x_1^{in} = 0$ (for AS) to $x_1^{in} = 0.225$ (maximal bending amplitude), except around $x_1^{in} = 0.115$ and $x_1^{in} = 0.217$.

In contrast to the SS-excitations, the stable area of phase space for bending oscillations is not small ($\pi/2 < \vartheta_{12} < 3\pi/2$ and $S_1^{max} \approx 1.73$) as can be seen from Figure 4, showing the Poincaré surface of section $\{(\vartheta_{12}, p_{\vartheta_{12}})|\alpha = \pi/4, p_\alpha > 0\}$ for asynchronous orbits with initial positions $x_1^{in} \in (0, 0.22)$. The POs with (rational) frequency ratios γ_1 composed of small integers can be recognized by the small number of fixed points appearing in the section. Some of these POs are shown in Figure 5. The winding numbers γ_2 of these POs can be obtain roughly from the Fourier transform of the $\mathcal{R}$-values at the intersection of the orbit with the surface $\alpha = \pi/4$, $p_\alpha > 0$. More accurate values can be extracted from the monodromy matrix [14] of the corresponding POs.

Since for these configurations $S_2 = 0$, the full action (4) calculated at $E = -1$ can be expressed as a function of S_1 only, *i.e.*, $S = S(S_1)$ and similarly $\gamma_{1,2} = \gamma_{1,2}(S_1)$. We have determined how the quantities S_1, S, γ_1 and γ_2 for the asynchronous orbits depend on the initial coordinate x_1^{in} by fitting numerical data[2] to the following polynomials

$$\begin{aligned} S_1 &= a\, x_1^{in}, \quad \text{(see Fig. 6)} \\ S &= S_0 + \sum_{i=1}^{4} b_i (x_1^{in})^i, \\ \gamma_{1,2} &= \gamma_{1,2}^{(0)} + \sum_{i=1}^{4} c_i^{(1,2)} (x_1^{in})^i, \end{aligned} \tag{5}$$

with the fitted coefficients summarized in Table 1.

[2] For S_1 we have used the areas enclosed by the curves corresponding to quasi-periodic orbits in the surface of section in Figure 4, whereas for S and $\gamma_{1,2}$ we have fitted the values for the POs.

Table 1. Coefficients for the fit of (5) (in atomic units at $E = -1$).

i	a	b_i	$c_i^{(1)}$	$c_i^{(2)}$
1	7.96146	−0.002961	0.422553	0.468802
2	–	1.900638	0.646674	2.551696
3	–	0.320787	1.317801	−16.676530
4	–	27.094104	6.141925	94.736750

The motion out of this subspace (*i.e.* the full three-dimensional) remains stable for small amplitudes of SS-excitations. This stable area changes in size (see Fig. 3) depending on the bending amplitude. For vanishing bending amplitude the corresponding stability island is shown in Fig. 2). Hence, the intra-shell (symmetrically-excited) states can be expected to be classically represented by regular motion in Ps^- since they have no SS-mode excitation (apart from zero-point motion). To obtain the spectrum one can apply torus quantization in contrast to the cases of He and H^-, where the corresponding classical orbits are unstable.

3.3 Near-separability and molecular-like behaviour

Since the size of the stable area around the AS orbit in the SS-direction is small, it follows that for all periodic orbits belonging to this area the hyperradius $\mathcal{R}$ changes only slightly. Taking the hyperradius as a measure for the size of a few-body system, we can conclude that the size of Ps^- in this area of phase-space is approximately constant. However, this does not imply a static configuration, rather intensive out-of-phase dynamics of the two electrons and the positron, from which in fact the stability of the configuration originates. Beside the hyperradius, the inter-electronic distance $R = r_{12}$ appears as an approximate constant (see Fig. 1c). This allows us to treat the collective motion of the three particles in Ps^- similarly to H_2^+ as it has been shown by the good agreement of full quantum calculations with the result from an adiabatic approximation (with R as the adiabatic variable) [7]. Moreover, the eigenfunctions are quasi-separable in prolate spheroidal coordinates $\lambda, \mu = (r_1 \pm r_2)/R$, ϕ (azimuthal angle) and can be described by the corresponding molecular-orbital (MO) quantum numbers n_λ, n_μ, m.

Here we demonstrate that the asynchronous orbits are the classical counterpart since they exhibit this quasi-separability as can be seen from Figures 5a–5f where the periodic orbits from Figures 5A–5F are shown in spheroidal coordinates.

Since the motion along λ (bending mode) and μ (AS-mode) is almost decoupled, the action S_1 should be approximately equal to the action of the (one-dimensional) λ-motion during two mean λ-periods

$$S_1 \approx 2\,\frac{S_\lambda(T)}{k_\lambda} \equiv 2\,S_\lambda, \tag{6}$$

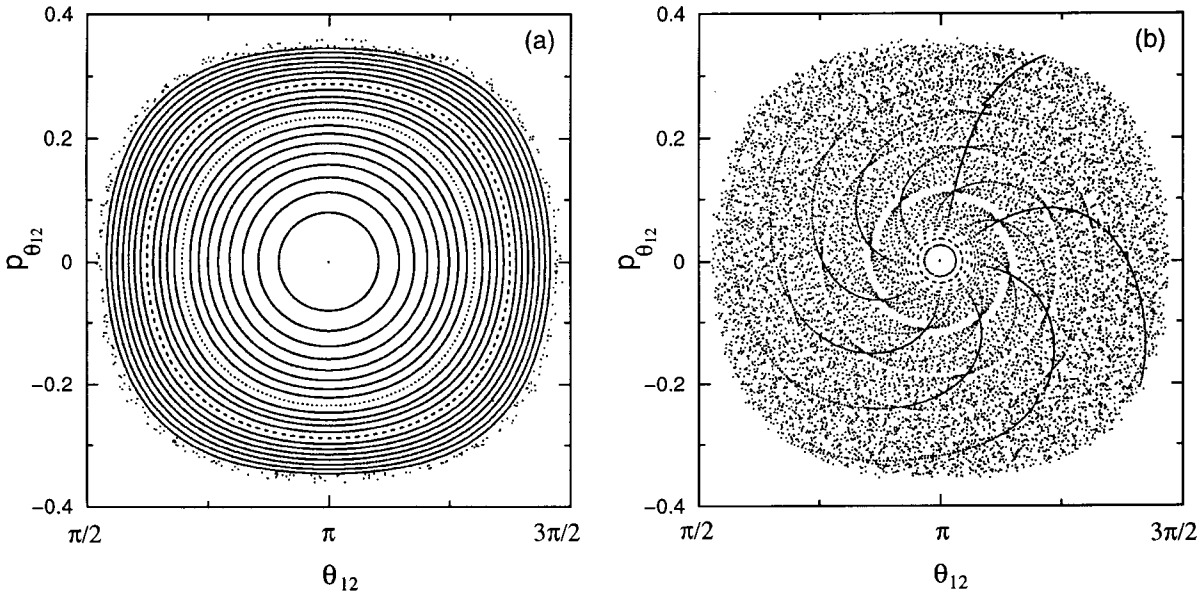

Fig. 4. Poincaré surface of section $\{(\vartheta_{12}, p_{\vartheta_{12}})|\alpha = \pi/4, p_\alpha > 0\}$ for asynchronous Ps^- configuration: (a) 23 orbits ($x_1 \in (0, 0.22)$, $t \leq 10\,000$); (b) 221 orbits ($x_1 \in (0, 0.22)$, $t \leq 200$).

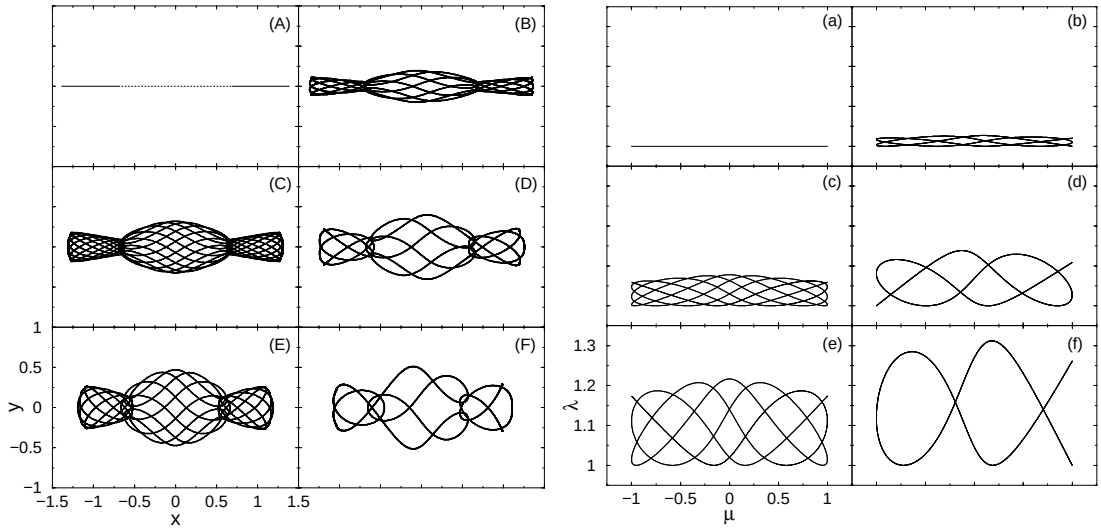

Fig. 5. (A–F) The asynchronous periodic orbits of the Ps^- ($E = -1$, $L = 0$) in the real space. The orbits are classified by the frequency ratio (winding number) of the bending and AS modes: $\gamma_1 = 1.11622$ (A), 9/8 (B), 8/7 (C), 7/6 (D), 6/5 (E), 5/4 (F). (a–f) Classical periodic orbits from the previous figure given in spheroidal coordinates. Using relation $\omega_\lambda/\omega_\mu = 2\gamma_1$ for the latest five orbits, it can be seen that $\gamma_1 = 9/8$ (b), 8/7 (c), 7/6 (d), 6/5 (e), 5/4 (f).

where $S_\lambda(T) = \int_{\mathrm{PO}} p_\lambda \, \mathrm{d}\lambda$ and k_λ is the number of oscillations performed by the λ-coordinate in the full period T of the corresponding PO[3]. The comparison between S_1 and S_λ in Figure 6 confirms the near-separability hypothesis. The near-separability, both of the wave-functions and the underlying classical dynamics, was demonstrated before for the intra-shell states of two-electron atoms [16,17]. For Ps^-, this separability provides an alternative way to perform the semiclassical quantization of the asynchronous configurations by applying the quantization conditions to the actions S_λ and S instead to S_1 and S to be discussed in the next section. Although this approach should be more approximate than the torus quantization almost the same results are obtained in the stable area due to (6). Moreover, it can be extended to the nearby chaotic area, because such weakly unstable configurations preserve the near-separability.

[3] Note that $\omega_\lambda = 2\omega_1$ since the motion in λ is doubly degenerate.

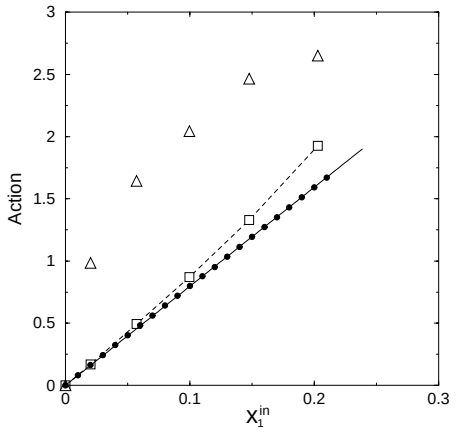

Fig. 6. The action S_1 (circles), calculated from the area enclosed by the curves from Figure 4a, for quasi-periodic motions on tori in the AS-bending subspace, and the ϑ_{12} and λ components of action integrals along the asynchronous POs accumulated during single ϑ_{12} and double λ mean periods – $S_{\vartheta_{12}}$ (triangles) and $2S_\lambda$ (squares), respectively. The actions are shown as functions of the initial values $x_1^{\rm in}$ for asynchronous trajectories lying on different tori. Due to the near-separability of the configuration in the prolate spheroidal coordinates, the values $2S_\lambda$ almost coincide with the corresponding values for the action variable S_1 (Eq. (5)).

4 Semiclassical quantization

Semiclassical torus quantization of the regular phase-space area of Ps^- requires to calculate the action integrals (3) and to apply the EBK quantum conditions

$$I_1' = 2\,(n_1 + 1/2), \quad I_2' = n_2 + 1/2, \quad I_3' = n_3 + 1/2. \quad (7)$$

The semiclassical quantum numbers n_1, n_2, n_3 are the numbers of nodes along the bending (doubly degenerate), SS and AS directions. Therefore, they coincide with the MO quantum numbers n_λ, ν and n_μ, respectively (here $m = 0$ since $L = 0$), and the action (4) is quantized according to

$$S' = 2\pi[n_\mu + 1/2 + \gamma_1(2n_\lambda + 1) + \gamma_2(\nu + 1/2)]. \quad (8)$$

The quantized energies of the system can be obtained by using the scaling relation $E' = -(S/S')^2$, which yields

$$E_{n_\mu,n_\lambda,\nu} = -\frac{(S/2\pi)^2}{[n_\mu + \gamma_1(2n_\lambda + 1) + \gamma_2(\nu + 1/2)]^2}\,. \quad (9)$$

In this formula the values for S and $\gamma_{1,2}$, for given quantum numbers, can be determined from the relations

$$\frac{S}{S_1} = \gamma_1 + \frac{n_\mu + 1/2 + \gamma_2(\nu + 1/2)}{2n_\lambda + 1}, \quad \frac{S_1}{S_2} = \frac{2n_\lambda + 1}{\nu + 1/2}, \quad (10)$$

which follow from $S/S_i = S'/S_i'$. In order to solve (10), we have to know how S and γ_i depend on S_1 and S_2.

Table 2. The action S_0 and the winding numbers γ_1^0, γ_2^0 of the collinear AS orbit, along with the effective central-particle charge $Z_{\rm eff}$ and the quantum defect μ which result from its semiclassical quantization (see Eqs. (11, 12)).

Sys.	S_0	$\gamma_1^{(0)}$	$\gamma_2^{(0)}$	$Z_{\rm eff}$	μ
He	22.986	1.0785	–	1.8292	$A/4-0.2893$
H^-	10.390	1.1712	–	0.8268	$A/4-0.3356$
Ps^-	7.2151	1.1162	0.6298	0.5742	$A/4-0.2156$

4.1 The intra-shell resonances associated with the near-collinear AS configuration

These are the resonances which have excitation only along the AS-orbit, *i.e.* $S \gg S_1, S_2$, or in terms of quantum numbers $n_\mu \neq 0$, but $n_\lambda = \nu = 0$. Although the quantum numbers for excitation perpendicular to the AS-orbit are zero, the zero point motion never renders the classical actions S_1 and S_2 exactly zero. Only in the asymptotic limit $N \gg 1$, the action S along the orbit is so much larger than S_1 and S_2 that we have practically $S = S_0$ and similarly we may approximate $\gamma_1 = \gamma_1^{(0)}$ and $\gamma_2 = \gamma_2^{(0)}$, where the sub/superscript zero denotes the values for the AS PO.

Then equation (9) reduces to a double Rydberg formula with principle quantum number N for both electrons,

$$E_N = -\frac{Z_{\rm eff}^2}{(N - \mu)^2}, \quad (11)$$

where $Z_{\rm eff} = S_0/4\pi$ and

$$\mu = [1 - \gamma_1^{(0)} + (A - \gamma_2^{(0)})/2]/2 \quad (12)$$

is the semiclassical expression for the quantum defect (see Tab. 2). It results from the decomposition of even and odd n_μ according to $n_\mu = 2N - 1 - (A + 1)/2$ (see *e.g.* [18]) where $A = 1$ for $^1S^e$ symmetry denoting an antinode at the line $r_1 = r_2$ while $A = -1$ is for $^3S^e$ with a nodal line at $r_1 = r_2$ [19]. Note that equation (12) differs from the one for He and H^- since for the latter ones $\mu = [(A + 1)/2 - \gamma_1^{(0)}]/2$ due to the instability of the SS-mode.

In the light of equation (11) the energy parameterized as $(-E_N N^2)^{-1/2}$ becomes a linear function of $1/N$ with different slope depending on A. This is shown in Figure 7 by full lines for the cases of helium and Ps^-. Towards the three-body breakup threshold $1/N \to 0$ the quantum-mechanical energies (parameterized as $(-E_N N^2)^{-1/2}$) approach these lines which demonstrates the applicability of the collinear AS model for $N \gg 1$.

For smaller N, the results from the AS collinear model deviate significantly from the exact quantum-mechanical values. Clearly, when N decreases, the zero-point motion of the other two modes becomes important compared to the AS-motion and thus the AS model is not a good approximation. In this case, one might expect that the semiclassical results can be improved if we consider the trajectories winding around the AS, *i.e.* if we take into account

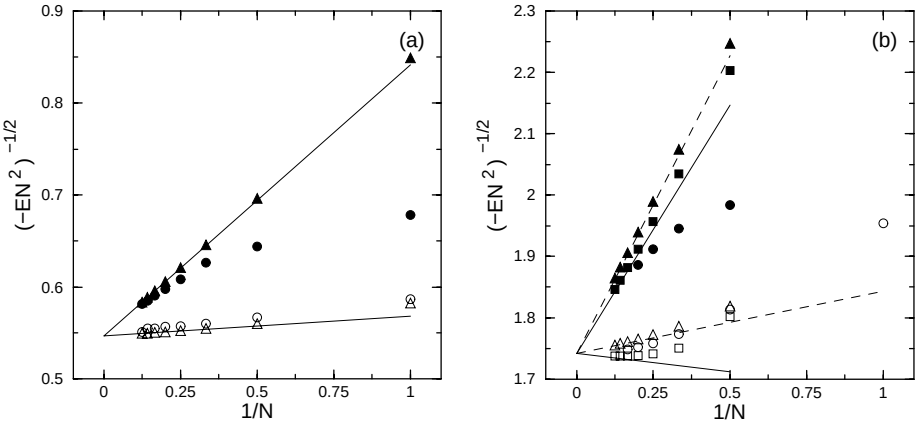

Fig. 7. Energies, parameterized as $(-E_N N^2)^{-1/2}$, of the lowest ($K_{\max}$) singlet (open symbols) and triplet (full symbols) resonant states in each manifold N, as functions of $1/N$ for: (a) helium and (b) Ps^-. The values from the exact quantum-mechanical calculations are represented by circles. The semiclassical results obtained using torus and WKB quantization are labeled by squares and triangles, respectively. The semiclassical values within the AS collinear model are shown by full lines, whereas the dashed lines correspond the latest model for Ps^-, treated analogously as helium (whose radial motion is unstable), *i.e.* taking formally $\gamma_2 = 1$.

that S, γ_1 and γ_2 depend on the actions S_1, S_2. However, the stable phase-space area in the SS-direction is very small as we have mentioned above, $S_2^{\max} \approx 0.009$ if $S_1 = 0$. A simple consideration using (10) with $n_\lambda = \nu = 0$ reveals that the states related to the stable classical motion are those with $N > 200$. This criterion for torus quantization, however, is not so strong in practice. The semiclassical results are acceptable already for $N \sim 10$ (see Tabs. 3 and 4) which is a consequence of the fact that the classical motion slightly outside of the stable area is still correlated in a similar way as inside, and the actions in (9) and (10) can be extrapolated to the nearby chaotic area.

4.2 The intra-shell resonances associated with off-collinear configurations

In the case of symmetrically excited states ($\nu = 0$) with $n_\lambda > 0$, the action S_1 is increasing (see Eq. (10)) and the AS collinear model is not a satisfying approximation. We have to go back to a larger phase space which is only reduced from the full phase space to planar configurations in the AS-bedding subspace (note that $S_2 \approx 0$ still holds by specifying intrashell states with $\nu = 0$). The parameters for the remaining asynchronous POs can be expressed in terms of S_1 only (see Eq. (5)) and the semiclassical formula for the energies of symmetrically excited Ps^- reads

$$E_{n_\mu, n_\lambda} = -\frac{(S/2\pi)^2}{[n_\mu + (1+\gamma_2)/2 + \gamma_1(2n_\lambda + 1)]^2}, \qquad (13)$$

where the values S, γ_1 and γ_2 are evaluated from the relation

$$\frac{S}{S_1} = \gamma_1 + \frac{n_\mu + (1+\gamma_2)/2}{2n_\lambda + 1}, \qquad (14)$$

using the empirically obtained functions $S = S(S_1)$, $\gamma_1 = \gamma_1(S_1)$, $\gamma_2 = \gamma_2(S_1)$ given implicitly by (5).

The size of the stable phase-space area restricts the applicability of equation (13). The range of stability in terms of relevant actions in (14) is given by

$$\frac{S(S_1^{\max})}{S_1^{\max}} - \gamma_1(S_1^{\max}) \approx 3 \qquad (15)$$

and for $N \gg 1$ we get from (13) the inequality $n_\mu/2n_\lambda > 3$. The criterion resumes a more accessible form if cast into group-theoretical quantum numbers[4], where it reads

$$K > N/2 \quad (N \gg 1). \qquad (16)$$

This means that the semiclassical quantization with (13) covers roughly one quarter of the states in each manifold N for which K can have different values $(-N+1, -N+3, ..., N-3, N-1)$.

As in the collinear case better results are obtained for higher values of N (Tabs. 3 and 4) since then it is less of an approximation to neglect the action of the zero point motion in the SS-mode.

4.3 WKB-quantization based on quasi-separability

For the ground and lower symmetrically-excited states of Ps^-, it is better to perform a WKB quantization based on the near-separability approximation than a torus quantization. This has been done for the unstable orbits of helium and H^-. In these cases the radial motion is more unstable than in Ps^- and it is not possible to treat the AS and SS modes independently (the winding number γ_2 is not defined). If we regard the region of stability as too small for quantization in Ps^- (see the discussion at the

[4] For relations between the MO and the group-theoretical quantum numbers, see [18].

Table 3. Energy levels for $^1S^e$ ($m = 0$, $A = +1$, $T = 0$) intra-shell ($\nu = 0$, $n = N$) resonant states of Ps^-, classified using MO and correlation quantum numbers. Semiclassical results obtained using the collinear AS and the planar asynchronous configuration (torus and WKB quantization) are given together with exact quantum mechanical values and those obtained within adiabatic molecular approximation [7]. The values denoted by an asterix are obtained extrapolating the action variable for bending mode S_1 slightly out of the stable area.

(n_μ, n_λ)	N	K	$E_{\rm SC}$(AS)	$E_{\rm SC}$(torus)	$E_{\rm SC}$(WKB)	$E_{\rm QM}$(exact)	$E_{\rm QM}$(MA)
(0, 0)	1	0	-0.3536		-0.2486	-0.2620	-0.2568
(2, 0)	2	1	-0.8533×10^{-1}	$-0.7702\times10^{-1*}$	-0.7557×10^{-1}	-0.7603×10^{-1}	-0.7512×10^{-1}
(4, 0)	3	2	-0.3748×10^{-1}	-0.3628×10^{-1}	-0.3483×10^{-1}	-0.3534×10^{-1}	-0.3511×10^{-1}
(2, 1)	3	0	-0.3471×10^{-1}		-0.2762×10^{-1}	-0.2774×10^{-1}	-0.2745×10^{-1}
(6, 0)	4	3	-0.2096×10^{-1}	-0.2062×10^{-1}	-0.1989×10^{-1}	-0.2021×10^{-1}	-0.2016×10^{-1}
(4, 1)	4	1	-0.1979×10^{-1}		-0.1748×10^{-1}	-0.1731×10^{-1}	-0.1719×10^{-1}
(8, 0)	5	4	-0.1337×10^{-1}	-0.1324×10^{-1}	-0.1283×10^{-1}	-0.1303×10^{-1}	-0.1303×10^{-1}
(6, 1)	5	2	-0.1277×10^{-1}	$-0.1203\times10^{-1*}$	-0.1177×10^{-1}	-0.1172×10^{-1}	-0.1169×10^{-1}
(4, 2)	5	0	-0.1220×10^{-1}		-0.9945×10^{-2}	-0.9824×10^{-2}	-0.981×10^{-2}
(10, 0)	6	5	-0.9263×10^{-2}	-0.9201×10^{-2}	-0.8957×10^{-2}	-0.9086×10^{-2}	-0.9107×10^{-2}
(8, 1)	6	3	-0.8913×10^{-2}	$-0.8455\times10^{-2*}$	-0.8396×10^{-2}	-0.8414×10^{-2}	-0.8384×10^{-2}
(6, 2)	6	1	-0.8581×10^{-2}		-0.7506×10^{-2}	-0.7438×10^{-2}	-0.7390×10^{-2}
(12, 0)	7	6	-0.6794×10^{-2}	-0.6762×10^{-2}	-0.6604×10^{-2}		-0.6717×10^{-2}
(10, 1)	7	4	-0.6573×10^{-2}	-0.6353×10^{-2}	-0.6273×10^{-2}		-0.6284×10^{-2}
(8, 2)	7	2	-0.6363×10^{-2}		-0.5784×10^{-2}		
(14, 0)	8	7	-0.5196×10^{-2}	-0.5177×10^{-2}	-0.5069×10^{-2}		-0.5156×10^{-2}
(12, 1)	8	5	-0.5047×10^{-2}	-0.4925×10^{-2}	-0.4858×10^{-2}		
(10, 2)	8	3	-0.4905×10^{-2}	$-0.4606\times10^{-2*}$	-0.4562×10^{-2}		
(16, 0)	9	8	-0.4101×10^{-2}	-0.4090×10^{-2}	-0.4013×10^{-2}		-0.4081×10^{-2}
(14, 1)	9	6	-0.3997×10^{-2}	-0.3923×10^{-2}	-0.3870×10^{-2}		
(12, 2)	9	4	-0.3897×10^{-2}	$-0.3619\times10^{-2*}$	-0.3678×10^{-2}		
(18, 0)	10	9	-0.3319×10^{-2}	-0.3312×10^{-2}	-0.3255×10^{-2}		-0.3101×10^{-2}
(16, 1)	10	7	-0.3243×10^{-2}	-0.3196×10^{-2}	-0.3154×10^{-2}		
(14, 2)	10	5	-0.3170×10^{-2}	-0.3035×10^{-2}	-0.3023×10^{-2}		
(20, 0)	11	10	-0.2742×10^{-2}	-0.2737×10^{-2}	-0.2694×10^{-2}		-0.2738×10^{-2}
(18, 1)	11	8	-0.2684×10^{-2}	-0.2653×10^{-2}	-0.2620×10^{-2}		-0.2634×10^{-2}
(16, 2)	11	6	-0.2629×10^{-2}	-0.2543×10^{-2}	-0.2525×10^{-2}		
(22, 0)	12	11	-0.2302×10^{-2}	-0.2299×10^{-2}	-0.2266×10^{-2}		-0.2302×10^{-2}
(20, 1)	12	9	-0.2258×10^{-2}	-0.2236×10^{-2}	-0.2210×10^{-2}		
(18, 2)	12	7	-0.2216×10^{-2}	-0.2157×10^{-2}	-0.2140×10^{-2}		
(24, 0)	13	12	-0.1961×10^{-2}	-0.1958×10^{-2}	-0.1932×10^{-2}		-0.1962×10^{-2}
(22, 1)	13	10	-0.1926×10^{-2}	-0.1911×10^{-2}	-0.1889×10^{-2}		
(20, 2)	13	8	-0.1893×10^{-2}	-0.1851×10^{-2}	-0.1836×10^{-2}		

end of Sect. 4.1) then, as in previous work for truly unstable orbits, instead of (13, 14) we should use

$$E_{n_\mu,n_\lambda} = -\frac{(S/2\pi)^2}{[n_\mu + 1 + \gamma_1(2n_\lambda+1)]^2}, \qquad (17)$$

$$\frac{S}{2S_\lambda} = \gamma_1 + \frac{n_\mu+1}{2n_\lambda+1}\ . \qquad (18)$$

Equations (17, 18) formally coincide with (13, 14) if we put $S_1 = 2S_\lambda$ and $\gamma_2 = 1$. From Table 3 it can be seen that, for smaller N, the WKB results for singlet states are in better agreement with quantum-mechanical results than those obtained using (13, 14). Moreover, the energy of the ground state is roughly correct. Contrarily, in the triplet case (Tab. 4) the off-collinear results appear even worse than those within the AS model. Note, however, that the energies in a manifold ($K = -N+1, ..., N-1$) are such as if they were shifted upwards by a constant (a similar effect has been observed for helium triplet states [4]). This indicates that the inaccuracy comes rather from an

Table 4. Same as in Table 3 but for $^3S^e$ ($m=0$, $A=-1$, $T=0$) intra-shell ($\nu=0$, $n=N+1$) resonant states.

(n_μ, n_λ)	N	K	$E_{\rm SC}$(AS)	$E_{\rm SC}$(torus)	$E_{\rm SC}$(WKB)	$E_{\rm QM}$(exact)	$E_{\rm QM}$(MA)
(3, 0)	2	1	-0.5423×10^{-1}	-0.5149×10^{-1}	-0.4948×10^{-1}	-0.6354×10^{-1}	-0.6328×10^{-1}
(5, 0)	3	2	-0.2745×10^{-1}	-0.2684×10^{-1}	-0.2582×10^{-1}	-0.2937×10^{-1}	-0.2919×10^{-1}
(7, 0)	4	3	-0.1653×10^{-1}	-0.1632×10^{-1}	-0.1579×10^{-1}	-0.1710×10^{-1}	-0.1701×10^{-1}
(5, 1)	4	1	-0.1570×10^{-1}		-0.1423×10^{-1}	-0.1586×10^{-1}	-0.1575×10^{-1}
(9, 0)	5	4	-0.1104×10^{-1}	-0.1095×10^{-1}	-0.1064×10^{-1}	-0.1124×10^{-1}	-0.1119×10^{-1}
(7, 1)	5	2	-0.1058×10^{-1}	$-0.9771\times10^{-2*}$	-0.9876×10^{-2}	-0.1053×10^{-1}	-0.1043×10^{-1}
(11, 0)	6	5	-0.7886×10^{-2}	-0.7842×10^{-2}	-0.7647×10^{-2}		-0.7947×10^{-2}
(9, 1)	6	3	-0.7610×10^{-2}	-0.7301×10^{-2}	-0.7221×10^{-2}		-0.7479×10^{-2}
(7, 2)	6	1	-0.7348×10^{-2}		-0.6571×10^{-2}		-0.6965×10^{-2}
(13, 0)	7	6	-0.5915×10^{-2}	-0.5890×10^{-2}	-0.5761×10^{-2}		-0.5942×10^{-2}
(11, 1)	7	4	-0.5735×10^{-2}	-0.5573×10^{-2}	-0.5498×10^{-2}		-0.5638×10^{-2}
(15, 0)	8	7	-0.4600×10^{-2}	-0.4585×10^{-2}	-0.4495×10^{-2}		-0.4614×10^{-2}
(13, 1)	8	5	-0.4476×10^{-2}	-0.4382×10^{-2}	-0.4322×10^{-2}		
(11, 2)	8	3	-0.4357×10^{-2}	$-0.4156\times10^{-2*}$	-0.4086×10^{-2}		
(17, 0)	9	8	-0.3679×10^{-2}	-0.3670×10^{-2}	-0.3605×10^{-2}		-0.3688×10^{-2}
(15, 1)	9	6	-0.3591×10^{-2}	-0.3532×10^{-2}	-0.3485×10^{-2}		
(13, 2)	9	4	-0.3505×10^{-2}	$-0.3328\times10^{-2*}$	-0.3327×10^{-2}		
(19, 0)	10	9	-0.3010×10^{-2}	-0.3004×10^{-2}	-0.2955×10^{-2}		-0.3016×10^{-2}
(17, 1)	10	7	-0.2944×10^{-2}	-0.2906×10^{-2}	-0.2868×10^{-2}		
(15, 2)	10	5	-0.2880×10^{-2}	-0.2774×10^{-2}	-0.2758×10^{-2}		
(21, 0)	11	10	-0.2508×10^{-2}	-0.2503×10^{-2}	-0.2466×10^{-2}		-0.2513×10^{-2}
(19, 1)	11	8	-0.2458×10^{-2}	-0.2431×10^{-2}	-0.2402×10^{-2}		-0.2431×10^{-2}
(17, 2)	11	6	-0.2409×10^{-2}	-0.2338×10^{-2}	-0.2321×10^{-2}		
(23, 0)	12	11	-0.2121×10^{-2}	-0.2118×10^{-2}	-0.2089×10^{-2}		-0.2126×10^{-2}
(21, 1)	12	9	-0.2082×10^{-2}	-0.2064×10^{-2}	-0.2040×10^{-2}		-0.2062×10^{-2}
(19, 2)	12	7	-0.2045×10^{-2}	-0.1995×10^{-2}	-0.1979×10^{-2}		

inadequate treatment of the chaotic radial motion than of the bending mode. The results by Wintgen *et al.* [6] for collinear helium support this conjecture. Semiclassical values for energies of this system obtained within the AS model deviate from the quantum-mechanical results more for triplet states than for singlet states. However, they can be significantly improved by including contributions of other collinear POs, using a variant of Gutzwiller's PO-theory [12] (the so-called "cycle-expansion" [3,6]), which is a more accurate semiclassical approach to chaotic motion.

5 Conclusions

In an exhaustive study of collinear and planar orbits in Ps^-, relevant for a semiclassical quantization of symmetrically excited states we have shown that that the planar, so-called asynchronous, orbits describe the off-collinear symmetrically excited ("intra-shell") resonances very well. They are the only simple classical objects known to represent these quantum resonances. In contrast to He or H^-, which have been studied previously, some of these orbits are stable. This fact allowed us to apply torus quantization and to study the role of stability for the quantization.

Particularly, the *highly* symmetrically-excited resonant states of Ps^- with $K = N/2, ..., N-1$ are related to the fully stable classical motion. This is confirmed by the fact that for $K = K_{\max}$ the semiclassical torus quantization which includes the contributions of all three stable modes (*i.e.* both winding numbers γ_1 and γ_2) yields results in better agreement with the quantum values than a semiclassical quantization assuming chaotic radial motion (where only γ_1 exists), as can be seen in Figure 7.

However, the small stability region around the asynchronous orbits in the symmetric stretch mode does not allow one to take efficiently advantage of this better classical description for quantization of the *lowest* intra-shell resonances compared to a description by the asymmetric stretch collinear orbit. Rather, it has turned out that the quasi-separability of the system in spheroidal coordinates is more important to obtain good semiclassical energies despite the presence of unstable classical motion.

Assuming quasi-separability one can use simply WKB quantization.

For higher excitation, we have obtained good agreement between the results from the torus quantization and from the WKB quantization based on the near-separability in molecular coordinates. This confirms the validity of the near-separability hypothesis and the molecular-like description for two-electron systems.

In contrast to the collinear asymmetric stretch, different planar orbits are used for different resonances. The properties of these orbits may change as a function of excitation energy. It could be interesting to see in future work if a change of these properties is reflected in a changing behavior of other observables (dipole excitation etc.) in the corresponding quantum states.

Appendix

To regularize the planar motion of the system given by Hamiltonian (1) we follow the procedure by Aarseth and Zare [10] and introduce regularized coordinates and momenta Q_k, P_k, $k = 1, 2, 3, 4$ by means of the transformations

$$\begin{aligned} x_1 &= Q_1^2 - Q_2^2, & y_1 &= 2Q_1Q_2, \\ x_2 &= Q_3^2 - Q_4^2, & y_2 &= 2Q_3Q_4, \\ p_{x_1} &= \frac{Q_1P_1 - Q_2P_2}{2R_1^2}, & p_{y_1} &= \frac{Q_2P_1 + Q_1P_2}{2R_1^2}, \\ p_{x_2} &= \frac{Q_3P_3 - Q_4P_4}{2R_2^2}, & p_{y_2} &= \frac{Q_4P_3 + Q_3P_4}{2R_2^2}, \end{aligned} \tag{A.1}$$

where $R_1^2 = r_1 = Q_1^2 + Q_2^2$, $R_2^2 = r_2 = Q_3^2 + Q_4^2$, and the new time variable τ by the transformation

$$\mathrm{d}t = R_1^2 R_2^2 \, \mathrm{d}\tau. \tag{A.2}$$

Then, the singularities in the Hamiltonian (1), where the old variables ($\mathbf{r}_i$, $\mathbf{p}_i$, t) are expressed in terms of the new ones (Q_k, P_k, τ), can be removed by defining a new Hamiltonian

$$\tilde{H} = R_1^2 R_2^2 (H - E) \equiv 0, \tag{A.3}$$

where E is the total energy of the system. With such transformed Hamiltonian $\tilde{H}$ the corresponding equations of motion preserve the canonical form and they are regular when $R_1 \to 0$ or $R_2 \to 0$. The new Hamiltonian has the explicit form

$$\begin{aligned} \tilde{H} = [&R_2^2\mathbf{P}_1^2 + R_1^2\mathbf{P}_2^2 + (Q_1^2P_1^2 - Q_2^2P_2^2)(Q_3^2P_3^2 - Q_4^2P_4^2) \\ &+ (Q_2^2P_1^2 + Q_1^2P_2^2)(Q_4^2P_3^2 + Q_3^2P_4^2)]/4 \\ &- R_1^2 - R_2^2 + R_1^2R_2^2(R_{12}^{-2} - E) \equiv 0, \end{aligned} \tag{A.4}$$

where $R_{12}^2 = r_{12} = [(Q_1^2 - Q_2^2 - Q_3^2 + Q_4^2)^2 + 4(Q_1Q_2 - Q_3Q_4)^2]^{1/2}$, $\mathbf{P}_1 = (P_1, P_2)$ and $\mathbf{P}_2 = (P_3, P_4)$. The limit $R_{12} \to 0$ is still singular. However, this is not relevant since this kind of collisions (electron-electron) never appears for relevant trajectories.

References

1. For a review, see G. Tanner, K. Richter, J.M. Rost, Rev. Mod. Phys. **72**, 498 (2000).
2. G. Tanner, D. Wintgen, Phys. Rev. Lett. **75**, 2928 (1995).
3. G.S. Ezra, K. Richter, G. Tanner, D. Wintgen, J. Phys. B: At. Mol. Opt. Phys. **24**, L413 (1991).
4. P.V. Grujić, N.S. Simonović, J. Phys. B: At. Mol. Opt. Phys. **28**, 1159 (1995).
5. N.S. Simonović, J. Phys. B: At. Mol. Opt. Phys. **33**, L85 (2000).
6. D. Wintgen, K. Richter, G. Tanner, Chaos **2**, 19 (1992).
7. J.M. Rost, D. Wintgen, Phys. Rev. Lett. **69**, 2499 (1992).
8. I.A. Ivanov, Y.K. Ho, Phys. Rev. A **61**, 2501 (2000).
9. L. Landau, E. Lifshitz, *Mechanics* (Nauka, Moscow, 1988), p. 35 (*in Russian*).
10. S.J. Aarseth, K. Zare, Celest. Mech. **10**, 185 (1974).
11. S. Watanabe, Phys. Rev. A **36**, 1566 (1987).
12. M.C. Gutzwiller, *Chaos in Classical and Quantum Mechanics* (Springer, New York, 1990).
13. J.M. Rost, R. Gersbacher, K. Richter, J.S. Briggs, D. Wintgen, J. Phys. B **24**, 2455 (1991).
14. N.S. Simonović, Chaos **9**, 854 (1999).
15. K. Richter, G. Tanner, D. Wintgen, Phys. Rev. A **48**, 4182 (1993).
16. J.M. Rost, R. Gersbacher, K. Richter, J.S. Briggs, D. Wintgen, J. Phys. B: At. Mol. Opt. Phys. **24**, 2455 (1991).
17. N.S. Simonović, J. Phys. B: At. Mol. Opt. Phys. **30**, L329 (1997).
18. J.M. Rost, J.S. Briggs, J. Phys. B: At. Mol. Opt. Phys. **24**, 4293 (1991).
19. C.D. Lin, Adv. At. Mol. Opt. Phys. **22**, 77 (1986).